

Performance of CFRP-Wrapped Connections

A. Parvin, & M. R. Blythe

Department of Civil Engineering, The University of Toledo, Toledo, Ohio, USA

Email: aparvin@eng.utoledo.edu

ABSTRACT: Externally-applied FRP wraps have proven to be efficient and effective technique to repair and strengthened structurally deficient beam-column joints. To date, the vast majority of FRP retrofitting studies have been performed on beams and columns. However, investigations on FRP strengthening of beam-column connections are scattered and limited. In the present study, interior and exterior as-built reinforced beam-columns joints are compared to their CFRP-wrapped counterparts through finite element analysis. The joints are subjected to constant axial and lateral cyclic loads. The lateral load versus displacement response of the interior joint control model was found to be superior to that of the exterior control joint model in all aspects. Therefore, the exterior T-joints are the more critical type to upgrade. However, regardless of their type, the CFRP-strengthened connections outperformed the as-built models in terms of strength and ductility.

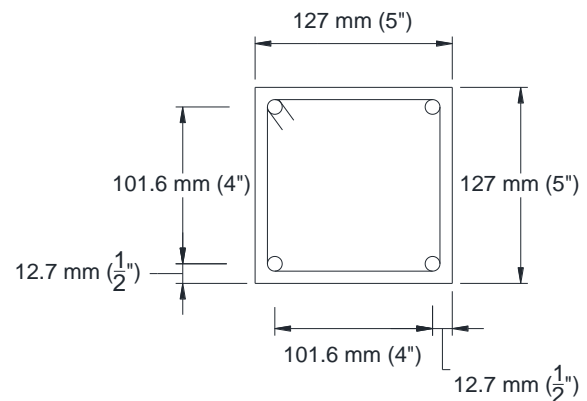
Keywords: Beam-columns, Joints, FRP-strengthening, Reinforced concrete, Finite element analysis

1 INTRODUCTION

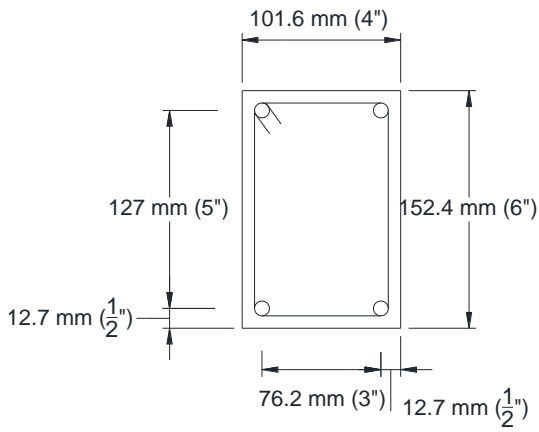
The use of fiber reinforced polymer (FRP) sheets to upgrade the susceptible beam-column connections is especially attractive in part due to FRP sheets' flexibility, non-corrosiveness, high strength-to-weight ratio, ease of application, and durability to environmental effects. As compared to beam and column members, FRP-strengthening of beam-column connections are scattered and limited due to their complexity (Antonopoulos and Triantafillou 2003; Ghojarah and Said 2001; Granata and Parvin 2001; Parvin and Wu 2008; Parvin et al. 2010). In the present study, interior and exterior as-built reinforced beam-columns joints are compared to their CFRP-wrapped counterparts through finite element analysis using Marc software program. The joints are subjected to constant axial and lateral cyclic loads and the effects of wrap on the strength, and ductility of upgraded joints are investigated.

2 FINITE ELEMENT MODELS OF EXTERIOR AND INTERIOR BEAM-COLUMN JOINTS

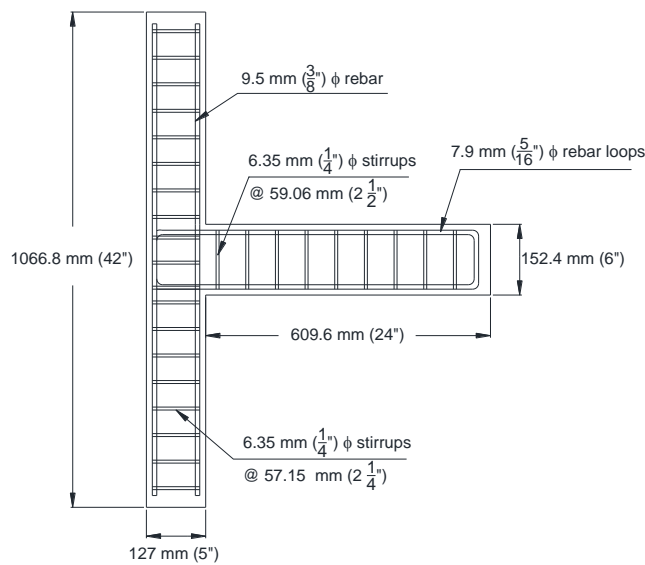
Four one-fourth scale exterior (T-shape) and interior (cross-shape) beam-column connections were modeled. The columns' height was 1067 mm (42 in) and the beams' length was 610 mm (24 in). Reinforcement details and dimensions of the joints' beams and columns are shown in Figure 1. The interior joint models were created by mirroring the beam dimensions and reinforcement presented in Figure 1 on both sides of the column.



(a) Column cross-section



(b) Beam cross-section



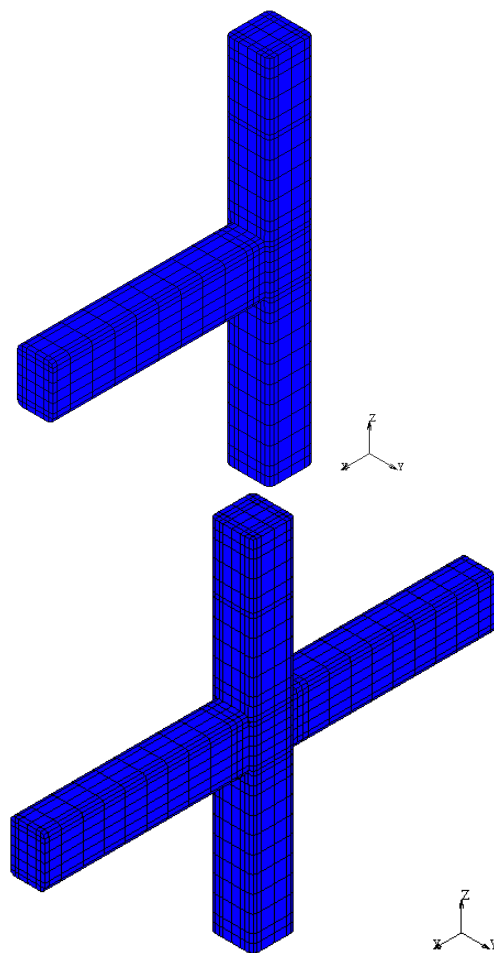
(c) Beam-column connection

Figure 1. Dimensions and reinforcement details

Summary of case studies of various connections are presented in Table 1. The control model refers to as-built joints, while the upgraded model refers to the joints that were strengthened using the CFRP sheets. Figure 2 represents the finite element models for both types of joints.

Table 1. Summary of case studies

Case No.	Joint Type	Joint Model
1	Exterior	Control
3	Exterior	Upgraded
4	Interior	Control
6	Interior	Upgraded



(a) Exterior joint model (b) Interior joint model

Figure 2. Finite element models of beam-column connections

Different element types were utilized in this study; solid for the concrete, truss for the steel reinforcement, and shell for the CFRP sheets. Every node of the rebar elements was attached to an associating node on a concrete element. The corners of beam and column elements were rounded at a radius of 12.7 mm (0.5 in). This was done to prevent high stress concentrations in the CFRP that are caused by sharp edges.

All concrete elements were considered to be isotropic with a modulus of elasticity of 20,683 MPa (3,000 ksi) and a Poisson's ratio of 0.17. The compressive strength was 27.6 MPa (4 ksi). Linear Mohr-Coulomb criterion in association with the combined work hardening rule was selected to govern the behavior of the concrete. The crushing of the concrete was modeled in Marc by selecting the cracking option and assigning a critical stress of 4.8 MPa (700 psi) and a crushing strain of 0.003. A softening modulus of 2.5 MPa (365 psi) was also assigned. This was done in order to allow the program to model the behavior of the concrete once cracks

occur. The softening modulus allows some strain to be carried across the crack.

All rebar elements were considered to be isotropic with a modulus of elasticity of 206,832 MPa (30,000 ksi) and a Poisson's ratio of 0.3. The yield strength was 413.6 MPa (60 ksi). Von Mises criterion in association with the combined hardening rule was chosen to govern the behavior of the rebar. The maximum tensile yield strain in all rebar elements was 0.002. The column rebar elements had a cross-sectional area of 71.0 mm² (0.11 in²), the beam rebar had a cross-sectional area of 49.7 mm² (0.077 in²), and the stirrup elements had a cross-sectional area of 31.6 mm² (0.049 in²).

The CFRP elements were considered to be orthotropic with a modulus of elasticity of 206,832 MPa (30,000 ksi) in the fiber direction. The Poisson's ratio was 0.22. The shear modulus was 3,447 MPa (500 ksi). The maximum tensile strain was set to 0.0106. It was assumed that the CFRP dominated the failure mode, so that the model failed once the CFRP failed.

A constant axial load of 6.9 MPa (1,000 psi) was applied to the top face of the column initially. This is representative of 0.25f_cAg and was kept the same for both the exterior and interior joints. The lateral cyclic load was applied to a 101.6 mm (4 in) x 190.5 (7 ½ in) area on the back face at the top of the column to simulate earthquake loading.

2.1 CFRP upgrade scheme

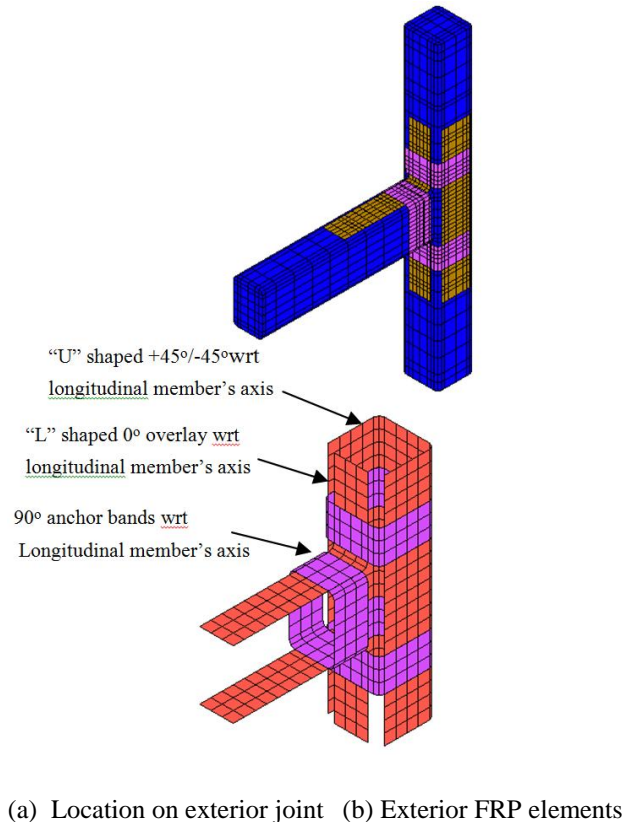
Figure 3 shows the developed CFRP-upgrade scheme for both exterior and interior joints. The CFRP upgrade scheme for the exterior joint consisted of one layer of +45° and one layer of -45° fibers with respect to the longitudinal axis of the column ("U" shape) and three layers of unidirectional fibers wrap used as transitional strips between the beam and the remaining face of the column ("L" shaped overlay). The transitional "L" elements were given a 12.7 mm (1/2 in) radius at the connection between the column and beam. Two layers of unidirectional fiber wraps (bands) were used to anchor both the +45°/-45° and transitional overlays to the column and the beam. These bands were applied over the top of the "U" and "L" overlays.

For the +45°/-45° overlay on the column in the areas that did not come into contact with the anchoring wraps, each layer was 0.18 mm (0.007 in) thick. This was modeled by assigning a thickness of 0.36

mm (0.014 in) to all of the shell elements. A composite material was then assigned to the elements that consisted of two layers with the first layer having fibers in the +45° direction and the second layer having fibers in the -45° direction.

The unidirectional transition strips were modeled by assigning a thickness of 0.53 mm (0.021 in) to the elements that composed of the part of the strips that were not overlapped by the anchoring strips. Each layer was 0.18 mm (0.007 in) thick. A composite material was assigned to these elements that composed of three layers, all of which had fibers in the 0° direction (parallel to the axial axes of the column and beam).

The anchoring wraps were broken down into three parts. The first set of anchoring wraps overlapped the +45°/-45° overlay on the column. These elements were assigned a thickness of 0.71 mm (0.028 in) to account for the two layers of column overlay and the two layers of anchor wraps. The composite material assigned to these elements consisted of one layer of fibers in the +45° direction, one layer in the -45° direction, and two layers in the 90° direction. The fiber directions were all with respect to the axial axes of the column and beam.



(a) Location on exterior joint (b) Exterior FRP elements

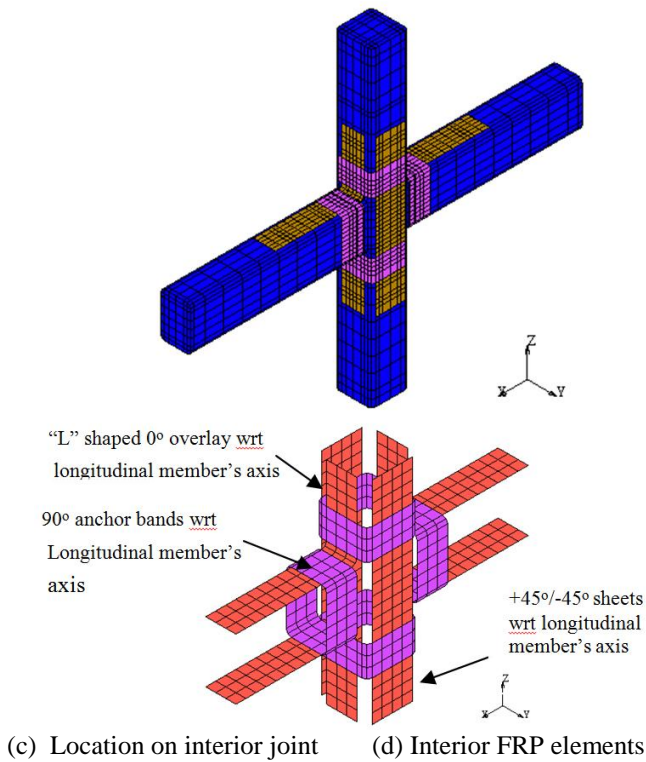


Figure 3. CFRP-upgrade scheme for beam-column connections

The second set of anchoring wraps overlapped the transition strips on the column and the beam. These elements were assigned a thickness of 0.89 mm (0.035 in) to account for the three layers of transitional overlay and the two layers of anchor wraps. The fibers of the transitional overlay ran parallel to the axial axes of the column and beam while the fibers of the anchor bands ran perpendicular to the axial axes of the column and beam. Therefore, the composite material assigned to these elements consisted of three layers of fibers in the 0° direction and two layers of fibers in the 90° direction. The fiber directions were set with respect to the axial axes of the column and the beam.

The third set of anchoring wraps overlapped concrete only. This occurred on the column between the $+45^\circ/-45^\circ$ overlay and the transitional strips and on the beam on the faces that did not have any overlay applied. These elements were assigned a thickness of 0.36 mm (0.014 in) to account for the two layers of anchor wraps. The composite material assigned to these elements consisted of two layers of fibers in the 90° direction (perpendicular to the axial axes of the column and beam).

The CFRP upgrade scheme for the interior joint was modeled similarly for the exterior joint. The main difference between the interior and exterior wrapping schemes is that, due to the additional beam in the interior joint, the one continuous $+45^\circ/-45^\circ$ overlay on three sides of the column ("U" shaped

overlay) is split into two individual $+45^\circ/-45^\circ$ overlays on the two opposite sides of the column (the sides with no beams). The upgrade scheme for the interior joint was modeled by mirroring the modeling of transition overlays and beam anchor strips of the beam in exterior joint to the additional beam in the interior joint. Since there were three layers of CFRP in the transitional overlays as opposed to the two layers in the $+45^\circ/-45^\circ$ overlay, the thickness of the column anchor strips was adjusted to accommodate the increase in thicknesses.

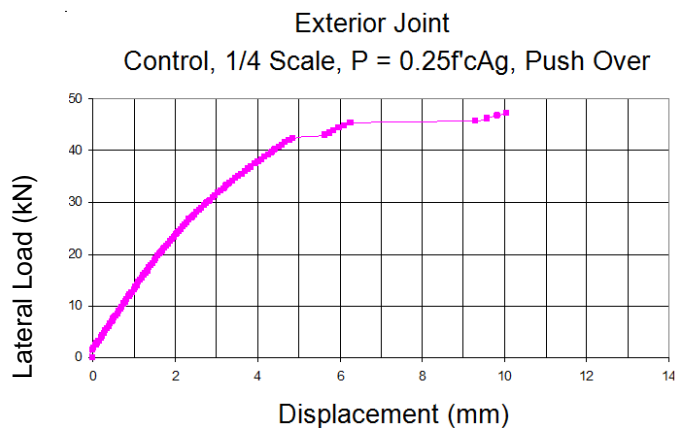
In the following sections results of exterior and interior control and CFRP-upgraded joints are discussed.

2.2 Exterior control joint (case 1)

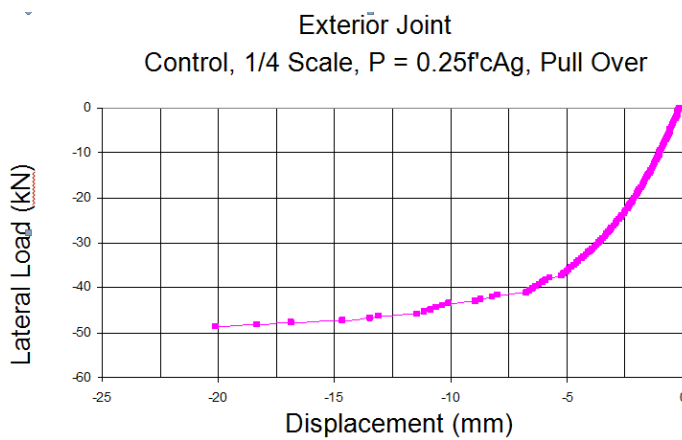
The exterior control joint consisted of 2142 solid elements to model the concrete and 788 truss elements to model the rebar. The compressive axial load base pressure applied was 6.9 MPa (1,000 psi). The lateral load base pressure applied was 2.4 MPa (350 psi), equivalent to $0.25f_cAg$.

In order to determine the ductility of the one-fourth exterior joints with an axial load of $0.25f_cAg$, prior to applying the seismic loading, both a positive and negative monotonically increasing load multiplier was applied to the lateral load base pressure in a separate run. These monotonically increasing tables simulated a push and pull over test. From Figure 4, it is apparent that the rebar yielded at a displacement of 4.9 mm (0.19 in) in push and 6.7 mm (0.26 in) in pull. The associated strain in the rebar at these displacements were approximately 0.002. This confirmed that the rebar yielded at these displacements. These values of yield displacements were then used to calculate the ductility of all of the one-fourth scale exterior joint models with an applied axial load of $0.25f_cAg$ through dividing the maximum displacement by the displacement at yield.

After the yield displacements were found, the cyclic lateral load was applied to simulate earthquake loading. The maximum loading for the control joint was 46.73 kN (10,505 lb) in both the push and pull load directions from Figure 5. The maximum displacement was 9.7 mm (0.38 in) in push and 15.1 mm (0.59 in) in pull directions with calculated ductility values of 1.99 and 2.25, respectively. The joint displaced a greater amount in the pull direction since the back side of the column did not have a beam to prohibit displacement.



(a) Positive monotonic load-displacement curve



(b) Negative monotonic load-displacement curve

Figure 4. Push/pull over results for exterior control joint (case 1)

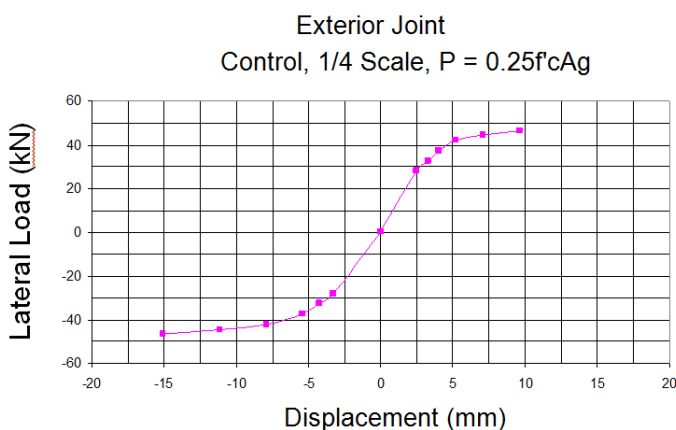


Figure 5. Load versus displacement envelope case 1

2.3 CFRP-upgraded exterior joint (case 3)

An additional 558 elements were used to model the CFRP sheets of upgraded exterior joint subjected to constant axial and lateral cyclic loads. As shown in Figure 6, the maximum load was 63.1 kN (14,185 lb) in both loading directions. The CFRP upgrade

scheme improved the maximum lateral load capacity of the exterior joint (case 1) by 35.0%. The maximum displacement was found to be 12.0 mm (0.47 in) in the push and 22.0 mm (0.87 in) in the pull directions with the associated ductility values of 2.46 and 3.28, respectively. The CFRP upgrade enhanced the ductility of the exterior control joint by 23.5% and 45.7% the push and pull directions, respectively. A summary of response of exterior beam-column joints is shown in Table 2. The CFRP upgrade enhanced the performance of the exterior joint in terms of lateral load, ductility and energy absorption capacity.

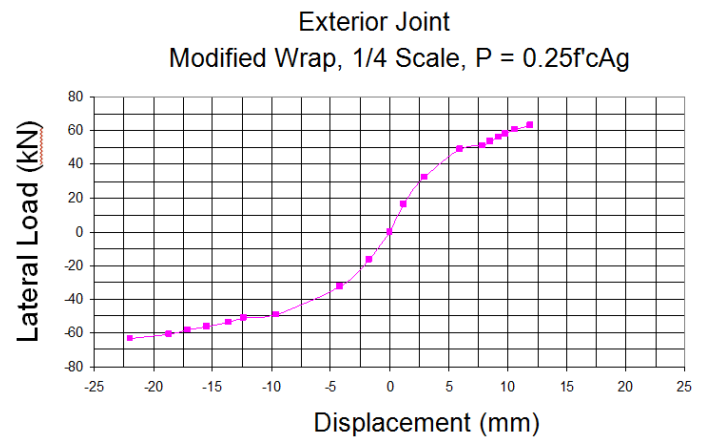


Figure 6. Load versus displacement envelope case 3

Table 2. Comparison of control and CFRP-upgraded exterior joints

Case No.	Model	Max Disp. (mm)	Max Load (kN)	Ductility Improvement Over Control		
				Disp. (%)	Load (%)	Ductility (%)
1	Control	9.67	46.73	1.99	-	-
		-15.08	-46.73	2.25	-	-
3	Up-graded	11.95	63.08	2.46	23.5	35.0
		-21.98	-63.08	3.28	45.7	35.0

2.4 Interior control joint (case 4)

The number of elements used to model the interior joint increased to 2,774 for concrete and 1,044 for rebar. The rebar yielded at a displacement of 4.53 mm (0.18 in) in both push and pull directions. The associated strain in the rebar at these displacements were approximately 0.002. This confirmed that the rebar yielded at these displacements. The additional beam of the interior joint stiffened the joint, and thus decreased the amount of displacement at yield by 6.8% in push and 32.5% in pull directions as compared to the exterior joint. These values of yield displacement were then used to calculate the ductility of all of the one-fourth scale interior joint models with an applied axial load of $0.25f_cAg$ through di-

viding the maximum displacement by the displacement at yield.

The maximum lateral load capacity in both load directions was 51.4 kN (11,555 lb) (see Figure 7). The additional beam increased the lateral load capacity of the joint by 10.0% as compared to the exterior control joint. The maximum displacement for the control joint was found to be 11.8 mm (0.47 in) in the push and 12.4 mm (0.49 in) in the pull directions. The maximum displacement for case 4 was 22.1% greater in pull and 17.9% less in push than the exterior control joint (case 1). The additional beam of the interior joint increased the ductility 31.0% in push and decreased the ductility 21.7% in pull compared to the associated exterior joint model (case 1). The overall response of the interior joint is more symmetric as opposed to that of the exterior joint due to the geometric symmetry. Even though the maximum displacement in the pull direction was decreased from that of the exterior joint, the associated ductility was increased. This was due to the reduction of the displacement at yield of the interior joint.

2.5 CFRP-upgraded interior joint (case 6)

A total of 600 elements were used to model the CFRP sheets for the interior joint. As shown in Figure 8, the maximum loading was found to be 65.4 kN (14,707 lb) in both push and pull directions. The modified wrap scheme improved the maximum load of the interior control model (case 4) by 27.3%, which was 7.7% less than the improvement the modified wrap scheme provided for the exterior joint (case 3). This was again due to the interior joint being initially stronger, thus the influence of the wrap was not as great as in the exterior joint.

The maximum displacement was found to be 15.6 mm (0.61 in) in the push and 14.7 mm (0.58 in) in pull directions. The associated ductility was 3.44 and 3.24, respectively. The CFRP upgrade scheme improved the ductility of the interior control joint (case 4) by 31.7% in push and 18.4% in the pull directions. These improvements were 8.2% greater in push and 27.3% less in pull than those of case 3. This can be attributed to the presence of the additional beam and the modification to the CFRP upgrade scheme in the exterior joint to accommodate the additional beam.

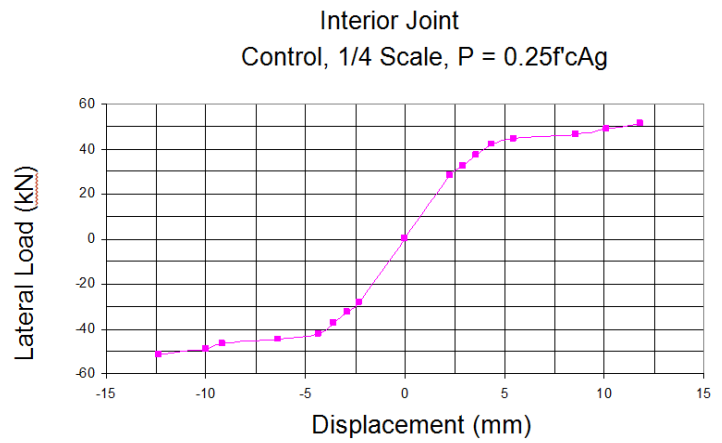


Figure 7. Load versus displacement envelope case 4

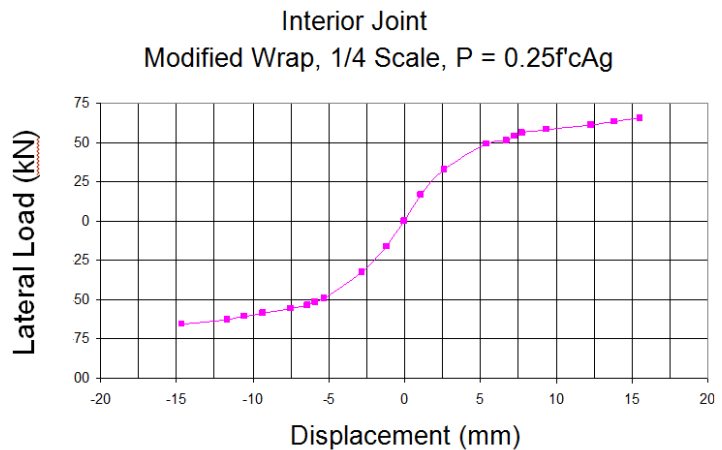


Figure 8. Load versus displacement envelope case 6

Table 3 shows a summary of cases 4 and 6. The higher improvement in the push direction of the CFRP-upgraded interior joint (case 6) over its exterior counterpart (case 3) is attributed to the additional strength provided by the additional beam while the less improvement in pull is attributed to the adjusted wrapping configuration required in order to accommodate the additional beam.

Table 3. Comparison of control and CFRP-upgraded interior joints

Case No.	Model	Max Disp. (mm)	Max Load (kN)	Ductility	Improvement Over Control		
					Disp. (%)	Load (%)	Ductility (%)
4	Control	11.81	51.40	2.61	-	-	-
		-12.38	-51.40	2.74	-	-	-
6	Up-graded	15.56	65.42	3.44	31.7	27.3	31.7
		-14.66	-65.42	3.24	18.4	27.3	18.4

3 CONCLUSIONS

Nonlinear finite element analysis models of exterior and interior control and CFRP-upgraded reinforced concrete beam-column connections were developed to examine their performance under axial and cyclic lateral load. The following conclusions were drawn from this study:

1. The CFRP-upgrade scheme increased the lateral load capacity by 27-35% and the maximum displacement by 18-45% of both the exterior and interior models as compared to the control joint counterparts.
2. The performance of the interior control joint surpassed that of the exterior joint (case 4 versus case 1). The lateral load capacity of the interior control joint was 10% greater than that of the exterior control joint. The ductility of the interior control joint was 31% greater in push and 22% greater in pull than that of the exterior control joint. Therefore the exterior "T" joints are the more critical type of joint to upgrade.
3. When comparing the exterior and interior joints, the amount of improvement that the upgrade scheme provided for the joint was affected by the presence of the additional beam in the interior joint.

4 REFERENCES

- Antonopoulos, C.P. and Triantafillou, T.C., "Experimental Investigation of FRP-Strengthened RC Beam-Column Joints," *J. Composites for Construction*, ASCE, V. 7, No. 1, 2003, pp. 39-49.
- Ghobarah, A. and Said, A., "Seismic Rehabilitation of Beam-Column Joints Using FRP Laminates," *J. Earthquake Engineering*, V. 5, No. 1, 2001, pp. 113-129.
- Granata, P.J. and Parvin, A., "An Experimental Study on Kevlar Strengthening of Beam Column Connections," *Composite Structures*, Vol. 53, No. 2, 2001 pp. 163-171.
- Parvin, A., and Wu, S., "Ply angle effect on fiber composite wrapped reinforced concrete beam-column connections under combined axial and cyclic loads," *Composite Structures*, Vol. 82, No. 4, 2008, pp. 532-538.
- Parvin, A., Altay, S. Yalcin, C., and Kaya, O., "CFRP Rehabilitation of Concrete Frame Joints with Inadequate Shear and Anchorage Details," *Journal of Composites for Construction*, ASCE, V. 14, No. 1, 2010, pp. 72-82.